Statistical Channel Modeling for Short Range Line–of–Sight Terahertz Communication

Kürşat Tekbıyık*†, Emre Ulusoy*†, Ali Rıza Ekti*‡, Serhan Yarkan§, Tunçer Baykaş¶, Ali Görçin*‖, Güneş Karabulut Kurt†
*Informatics and Information Security Research Center (BİLGEM), TÜBİTAK, Kocaeli, Turkey
†Department of Electronics and Communication Engineering, Istanbul Technical University, İstanbul, Turkey
‡Department of Electrical–Electronics Engineering, Balıkesir University, Balıkesir, Turkey
§Department of Electrical–Electronics Engineering, Istanbul Commerce University, İstanbul, Turkey
¶Department of Electrical–Electronics Engineering, Medipol University, İstanbul, Turkey
‖Faculty of Electronics and Communications Engineering, Yıldız Technical University, İstanbul, Turkey
Emails: {kursat.tekbiyik, emre.ulusoy}@tubitak.gov.tr, arekti@balikesir.edu.tr, syarkan@ticaret.edu.tr, tbaykas@medipol.edu.tr, agorcin@yildiz.edu.tr, gkurt@itu.edu.tr

***Abstract*—Underutilized spectrum constitutes a major concern in wireless communications especially in the presence of legacy systems and the prolific need for high–capacity applications as well as consumer expectations. From this perspective, Terahertz frequencies provide a new paradigm shift in wireless communications since they have been left unexplored until recently. Such a vast frequency spectrum region extending all the way up to visible light and beyond points out significant opportunities from dramatic data rates on the order of tens of Gbps to a variety of inherent security and privacy mechanisms, and techniques that are not available in the traditional systems. Thus, in this paper, we investigate statistical parameters for short–range line–of–sight channels of Terahertz communication. Short–range measurement campaign within the interval of [3cm, 20cm] are carried out between 275GHz to 325GHz range. Path loss model is examined for different frequencies and distances to provide the insight regarding the effect of the operating frequency. Measurement results are provided with relevant discussions and future directions.**

***Index Terms*—Terahertz channel modeling, short range terahertz communication**

I. Introduction

Mobile data traffic has exploded exponentially within the past years which which most of the data is generated by wireless devices [1]. One should note that number of users, devices and services are also escalated along with the volume of data traffic [2]. In addition to this, market targets data rates approaching tens of Gbps even Tbps within next 10 years [3, 4]. Clearly, such high rates can only be accomplished by spectral efficient modulation types and/or increasing the transmission bandwidth significantly. Thus, Terahertz (THz) spectrum is considered to be a very promising solution for spectrum underutilization. On–board chip–to–chip communications, booth downloading, machine–to–machine (M2M) communications as well as wireless backhauling are just to name a few of the potential applications of THz communication system [4–7]. However, there are certain technical concerns regarding THz communication systems to ramp up in the near future such that realization of fully operational THz communications systems requires to fulfill multi–disciplinary efforts including statistical channel characterizations, advanced transceiver designs and signal processing techniques. Foremost among these techniques is establishing a well–defined statistical channel models.

A. Related Work

In literature channel modeling can be divided into several categories such as measurement methodology, frequency, spatial domains and application specific. For ray tracing, several parameters should be predefined such as path loss, angle of arrival, size and shapes of the measurement environment [8, 9]. In [10, 11], the THz band channel is analyzed in terms of spatial and temporal characteristics for short–range indoor communication. However, any changes within the measurement environment require to redo the calculations and bring a huge burden in regards to computational time. Therefore, a set of well–defined stochastic approach based measurement strategies should be employed due to the practical concerns.

For example, in [12], entire THz band measurement data set is split into smaller parts and then post–processed. One should note that such a strategy can create artifacts during the concatenation. The channel characteristics for 2×2 multiple–input multiple–output (MIMO) line–of–sight (LOS) systems operating at THz region are presented in [13, 14]. However, there is a significant conflict between the theoretical rates and measurement results. The distinct features of three dimensional (3D) THz channels are studied in terms of array steering vector and path gain by utilizing ultra–massive MIMO systems [15–17]. Under the LOS condition, [18] showed that attenuation factor can be modeled as a Rician or Nakagami–m distribution. Besides traditional channel measurements, scenario–specific measurement results which considers two dimensional (2D) geometrical propagation model for short–range device–to–device (D2D) desktop communication channels in the presence of multipath fading is investigated in [19].

Based on the aforementioned studies, one should conclude that further analyses for short–range communication channels at THz bands are required in order to come up with a solid statistical propagation channel model. Moreover, measurement campaigns and methods should be diversified since equipment employed in data collection manifest dramatic limitations under certain conditions. In contrast to our previous work in [18], a short–range THz propagation channel measurement campaign is established in a fully anechoic chamber. The contributions of this study is two–fold. To the best knowledge of authors, this study is the first in short–range THz propagation channel measurements where data are collected with the use of all–electronic (no optical) components and extenders in time–domain. Second, a generic log–linear path loss for LOS path is proposed with a two–slope extension. Results are provided along with relevant discussions.

B. Paper Organization

The remainder of this paper is organized as follows. Section II details the signal model. The measurement setup is explained in Section III. In Section IV, measurement results are given and discussed. Finally, Section V concludes the paper.

II. Statistical Characterization of Terahertz Channel: Signal Model

We consider a LOS short–range THz communication which takes place in the distance interval between [3cm, 20cm] for the frequency range of 275GHz to 325GHz as shown in Fig. 1 and given in details in Section III.

The received signal at passband is given as:

$$r(t) = \mathrm{Re}\left\{\left(x_I(t) + jx_Q(t)\right)e^{j2\pi f_c t}\right\} \tag{1}$$

where $x_Q(t)$ and $x_I(t)$ denotes the quadrature and in–phase components of the transmit baseband signal, respectively; $j = \sqrt{-1}$; $\mathrm{Re}\{\cdot\}$ stands for the real part the signal; f_c is the transmission frequency. Under the LOS condition, the complex baseband of the channel can be simplified as[1]:

$$h(t) = a_f e^{j\theta}\delta(t - t_0) \tag{2}$$

where θ denotes the phase; a_f emblematises the amplitude of LOS path with respect to the specular power because of the environment geometry; t_0 represents the propagation delay which is equal to d/c where c and d is the speed of light and the distance between the receiver and transmitter, respectively. Common practice for the THz communications is to use the directional antennas,

[1]The number of resolvable multipath component is equal to 1 for short–range LOS Terahertz communications.

Fig. 1. Two perspectives for the measurement setup in anechoic chamber. LOS conditions are guaranteed by isolating measurement setup and employing anechoic chamber.

therefore, the impact of antenna misalignment; frequency dispersion index; and frequency–dependent loss can all be combined and shown as a_f.

Measurement setup described in Section III does not allow non line–of–sight (NLOS) transmission due to the absorbers and full isolation in an anechoic chamber. As a result, the contribution of path loss to the term a_f in (2) is given by:

$$PL = PL_0 + 10\gamma\log_{10}(d) \tag{3}$$

where PL_0 stands for the path loss at a reference distance for antenna far field; γ denotes the path loss coefficient; d is the distance between transmitter and receiver.

III. Terahertz Measurement Setup

A. Description of The Measurement Setup

An experimental measurement setup was constructed in the Millimeter Wave and Terahertz Technologies Research Laboratories (MİLTAL) at the Scientific and Technological Research Council of Turkey (TÜBİTAK) in Gebze, Turkey and Fig. 1 shows the measurement setup in anechoic chamber. The length, width, and height of the anechoic chamber are 7m, 3m, and 4m, respectively.

The measurement setup includes five main equipment: Oleson Microwave Labs (OML) V03VNA2–T, Agilent performance network analyzer (PNA) vector network analyzer (VNA) E8361A, Rohde & Schwarz SMT20 20GHz signal generator, Rohde & Schwarz FSW26 signal and spectrum analyzer (SSA), OML V03VNA2–T/R–A millimeter wave extender modules and N5260A extender controller. Maximum measurement frequency of the VNA is 67GHz, so in order to generate the local oscillator (LO) signals from 275GHz to 325GHz, the 220GHz to 325GHz extender modules are used with the VNA using the N5260A extender controller to analyze channel behaviours at sub-THz region. V03VNA2–T/R–A extender module consists of multipliers ($\times 18$) that upconverts radio frequency (RF) input signals in between 12.2GHz and

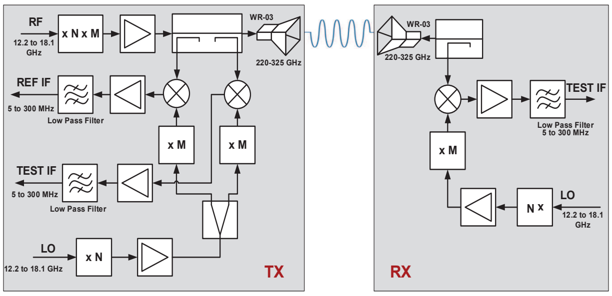

Fig. 2. Block diagram of the measurement setup.

18.1GHz to the band from 220GHz to 325GHz frequency range. Test intermediate frequency (IF) and reference IF signals at the transmitter side are monitored and checked by using down–conversion mixers before transmitting to ensure the validity of measurement. After propagation in the wireless THz channel, the received signal is down–converted at the receiver module, V03VNA2–R, by using down–conversion mixers and the resulting test IF (5MHz to 300MHz) signal at the receiver side is forwarded to the SSA. The channel characteristics are analyzed by monitoring the transmitted and down–converted pulse modulated signals at the SSA. Fig. 2 shows the corresponding block diagram of measurement setup.

The 220GHz to 325GHz source modules consist of balanced multipliers, which are driven by an extended band WR–10 multiplier chain with a WR–03 waveguide output interface. The output source match between the modules is typically 9dB. The measurements are taken with a continuous wave (CW) LO signal generated by the VNA and a CW modulated RF drive signal generated by the signal generator. In order to operate OML modules, $+10$dBm RF and LO signal power is required. The system has the dynamic range of 75dB (min. 60dB). Also, the WR–03 waveguide of the V03VNA2–T/R–A provides output power around -23dBm. The phase and magnitude stability of the extender modules are $\pm 8^\circ$ and ± 0.4dB, respectively.

B. Measurement Methodology

In this study, 275GHz to 325GHz is intentionally focused to achieve high performance from the extender modules, from the point of magnitude and phase stability of LO signal. By recording I/Q samples utilizing the measurement setup shown in Fig. 1 and Fig. 2, channel transfer function is obtained. The mismatches caused by the components is removed by calibrating the measurement system consisting of connectors and cables. The waveguide ports of the transmitting and receiving extender module with 100Hz IF bandwidth are directly interconnected to calibrate the measurement system. During the measurements, standard gain horn antennas with 24.8dBi gain at the center frequency are employed at both

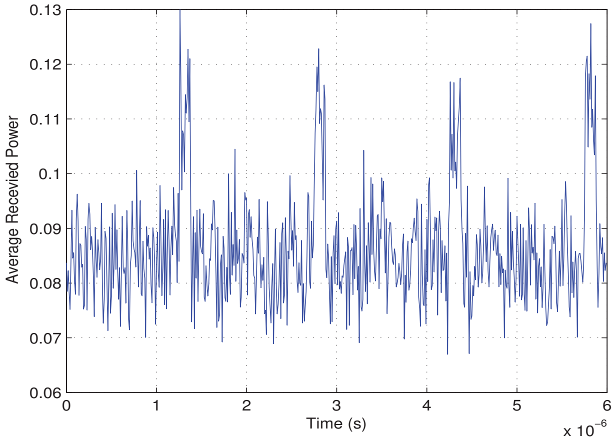

Fig. 3. A snapshot of pulse train measurement. Four consecutive pulses could be seen clearly in the snapshot.

the transmitter and receiver. Full 50GHz channel band measurements are based on the pulse modulated signals driven by the signal generator. The width of the pulse is 140ns and this pulse signal has a bandwidth around of 71MHz. Using SSA, each measurement is recorded with 100000 I/Q samples for a length of 1ms. I/Q sampling rate implies that the analysis bandwidth of the receiver covers the bandwidth of the transmitted pulse. The I/Q data is stored in the internal memory of the Rohde & Schwarz SSA. Then, the I/Q data is transferred into a personal computer on which MATLAB software runs for post-processing by using an external universal serial bus (USB) storage device.

IV. Measurement Results

In the literature, THz propagation channel measurements could be established majorly by frequency sweep technique especially when mmWave/sub–mmWave VNAs are employed. Devices that use high–order extenders are not preferred in pulse measurements due to their operational limitations. In contrast to the studies present in the literature, this study focuses on pulse measurements with the use of extenders and mmWave VNA. Considering the low–fidelity problem, validity of measurements should be checked. Fig. 3 depicts a snapshot of such a test measurement where each and every single pulse falling into the observation window could easily be observed. However, the fidelity of the pulses such as their periodicity and widths should be investigated further. Upon post–processing the test measurement, periodicity and width of the pulses are verified and validated with the use of statistical signal processing techniques and measurement campaign is then initialized.

In this study, measurement campaign focuses in the following aspects: First, how the received power is related to the transmitter–receiver separation. Second, how the received power is related to the frequency band. In order to observe these two aspects simultaneously, Fig. 4 could be investigated. In the figure, it is evident that the received power decreases with the transmitter–receiver separation, as expected. Another important observation is that some frequency bands in THz region behave quite differently in comparison with the ultra high frequency (UHF) bands. For instance, in Fig. 4, one could identify that 280GHz band is followed by 320GHz in terms of the least amount of loss introduced by the propagation channel.

As can be identified clearly from Fig. 4, there is a pattern in how the frequency affects the received power regardless of the transmitter–receiver separation. Moreover, the impact of the frequency is more pronounced for transmitter–receiver separations of 3cm and of 5cm. Further transmitter–receiver separations dominate this pattern due to path loss. For instance, operating frequency introduces a loss more than 6dB in case 305GHz is selected rather than 280GHz for a transmitter–receiver separation of 3cm. Nevertheless, the impact of operating frequency is not that dramatic for transmitter–receiver separations which are greater than 10cm.

In light of the discussion above, one could focus on solely path loss once an operating frequency is decided. Considering the fact that energy spreads over a volume in an exponentially decaying way, generally linearized version of the power loss with respect to transmitter–receiver separation is used. Measurement results reveal that THz channels obey the linear path loss with $PL = 0.224 - 9.014d$ where d denotes the transmitter–receiver separation. Both measured data and corresponding model fit could be seen in Fig. 5. Due to the extremely wide bandwidth, this model could be fine–tuned based on a frequency dependency, which seems to be more realistic as discussed above. Furthermore, as mentioned before, a transmitter–receiver separation of 10cm manifests a breaking point for almost all of the operating frequencies considered. Hence, a two–slope model could be investigated as well. When least–squares estimation is applied to the measurement data, the following path loss model is obtained:

$$PL = \begin{cases} 0.37 - 11.7d & , d \in (0, 0.1)\text{m} \\ -0.09 - 7.11d & , d \in [0.1, 0.2)\text{m} \end{cases} \quad (4)$$

The two–slope model obtained for the measurement data could be seen in Fig. 5 labeled as “first” and “second” slopes, respectively.

V. Concluding Remarks and Future Directions

THz communications are great prospect to use for short–range infotainment systems, which suggest that within a residential setting the locations of THz devices can be random. In this regard, THz measurements require an extra depth of planning in contrast to conventional propagation channel measurements since measurement

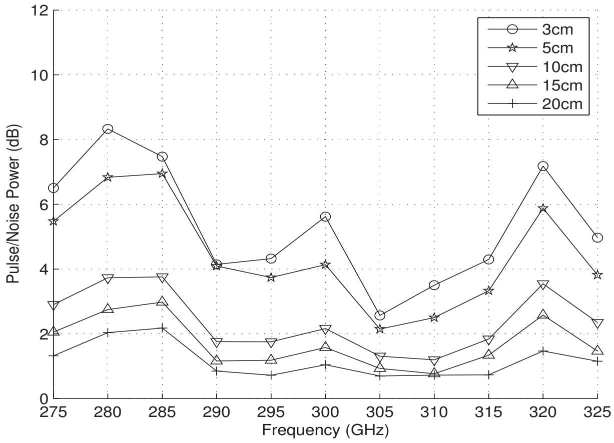

Fig. 4. Pulse power over noise power for various distances with respect to frequency bands.

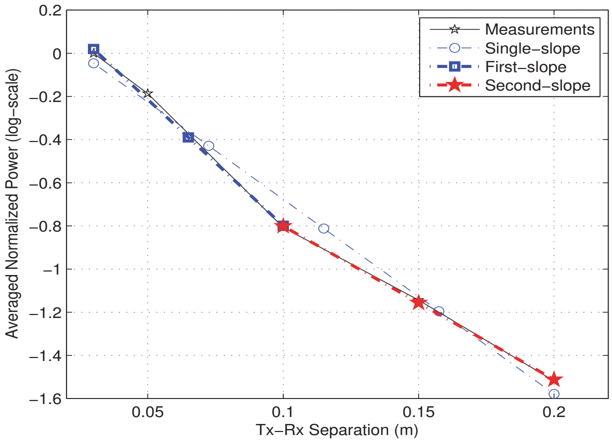

Fig. 5. Normalized received power averaged over frequencies with respect to transmitter–receiver separations.

duration, measurement methodology, measurement campaign, and post-processing time are prominent parameters to be taken into account. It is obvious that each and every item in this list corresponds to a specific set of scenarios. Considering the fact that a successful communication system relies totally on analyzing the statistical characteristics of the channel and employing the optimum transceiver algorithms, each set of environment with each and every set of conditions for almost all possible transceiver interactions constitute a significant duration, effort, and processing power.

One of the most important observations obtained from measurements is that optimal received power calculation should rely not only on transmitter–receiver separation but also on the frequency. Even though the transmitter–receiver separation introduces an exponential decrease into received power, operating frequency manifests totally different behavior on the received power. Therefore, a joint approach including both transmitter–receiver separation and operating frequency should be adopted for appropriate modeling the THz bands.

Another interesting finding is that short–range THz bands could be better modeled with two–slope path loss for free–space propagation. Measurement results reveal that a transmitter–receiver separation of 10cm yields a significant drop in the received power which implies the necessity of including a breaking point in the model. Such a result might indicate a ranging mechanism for any transmitter–receiver pair that intends to communicate through the use of THz bands.

REFERENCES

[1] Cisco, "White Paper: The Zettabyte Era-Trends and Analysis," Available: http://www.cisco.com/c/en/us/solutions/collateral/service-provider/visual-networking-index-vni/vni-hyperconnectivity-wp.pdf, Accessed: Apr. 18, 2017.

[2] W. W. R. Forum, "Visions and Research Directions for The Wireless World: Multi–RAT Network Architecture," Available: http://www.wwrf.ch/files/wwrf/content/files/publications/outlook/Outlook9.pdf, Accessed: Apr. 18, 2017.

[3] T. Schneider, "Ultrahigh-Bitrate Wireless Data Communications via THz-Links; Possibilities and Challenges," *J. Infrared Milli. Terahz. Waves*, vol. 36, no. 2, pp. 159–179, Feb. 2015.

[4] I. F. Akyıldız, J. M. Jornet, and C. Hana, "Terahertz band: Next frontier for wireless communications," *Physical Communication*, vol. 12, pp. 16–32, Sep. 2014.

[5] T. Kürner and S. Priebe, "Towards THz Communications - Status in Research, Standardization and Regulation," *J. Infrared Milli. Terahz. Waves*, vol. 35, no. 1, pp. 53–62, Jan. 2014.

[6] T. Tajima, T. Kosugi, H.-J. Song, H. Hamada, A. E. Moutaouakil, H. Sugiyama, H. Matsuzaki, M. Yaita, and O. Kagami, "Terahertz MMICs and Antenna-in-Package Technology at 300 GHz for KIOSK Download System," *J. Infrared Milli. Terahz. Waves*, vol. 37, no. 2, pp. 1213–1224, Dec. 2016.

[7] H.-J. Song, H. Hamada, and M. Yaita, "Prototype of KIOSK Data Downloading System at 300 GHz: Design, Technical Feasibility, and Results," *IEEE Commun. Mag.*, vol. 56, no. 6, pp. 130–136, 2018.

[8] S. Priebe and T. Kürner, "Stochastic Modeling of THz Indoor Radio Channels," *IEEE Trans. Wireless Commun.*, vol. WC-12, no. 9, pp. 4445–4455, Sep. 2013.

[9] D. He, K. Guan, A. Fricke, B. Ai, R. He, Z. Zhong, A. Kasamatsu, I. Hosako, and T. Krner, "Stochastic channel modeling for kiosk applications in the terahertz band," *IEEE Transactions on Terahertz Science and Technology*, vol. 7, no. 5, pp. 502–513, Sep. 2017.

[10] R. Piesiewicz, T. Kleine-Ostmann, N. Krumbholz, D. Mittleman, M. Koch, J. Schoebei, and T. Kurner, "Short-range ultra-broadband terahertz communications: Concepts and perspectives," *IEEE Trans. Antennas Propag.*, vol. 49, no. 6, pp. 24–39, 2007.

[11] S. Nie and I. F. Akyildiz, "Three-dimensional dynamic channel modeling and tracking for terahertz band indoor communications," in *2017 IEEE 28th Annual International Symposium on Personal, Indoor, and Mobile Radio Communications (PIMRC)*, Oct 2017, pp. 1–5.

[12] N. Khalid and O. B. Akan, "Wideband THz Communication Channel Measurements for 5G Indoor Wireless Networks," in *Proc. IEEE 2016 ICC Int. Conf. Commun.*, Kuala Lumpur, Malaysia, Jul. 2016, pp. 1–6.

[13] Z. Xu, X. Dong, and J. Bornemann, "Design of a Reconfigurable MIMO System for THz Communications Based on Graphene Antennas," *IEEE Trans. Terahertz Sci. Technol.*, vol. 4, no. 5, pp. 609–617, 2014.

[14] N. Khalid and O. B. Akan, "Experimental Throughput Analysis of Low-THz MIMO Communication Channel in 5G Wireless Networks," *IEEE Wireless Commun. Lett.*, vol. WCL-5, no. 6, pp. 616–619, Dec. 2016.

[15] I. F. Akyildiz and J. M. Jornet, "Realizing Ultra–massive MIMO (1024× 1024) Communication in the (0.06–10) Terahertz Band," *Nano Commun. Netw.*, vol. 8, pp. 46–54, 2016.

[16] L. Zakrajsek, E. Einarsson, N. Thawdar, M. Medley, and J. M. Jornet, "Design of Graphene–based Plasmonic Nano–antenna Arrays in The Presence of Mutual Coupling," in *11th European Conference on Antennas and Propagation (EuCAP)*. IEEE, 2017, pp. 1381–1385.

[17] C. Han, J. M. Jornet, and I. Akyildiz, "Ultra–Massive MIMO Channel Modeling for Graphene–Enabled Terahertz–Band Communications," in *87th Vehicular Technology Conference (VTC Spring)*. IEEE, 2018, pp. 1–5.

[18] A. R. Ekti, A. Boyaci, A. Alparslan, I. Unal, S. Yarkan, A. Gorcin, H. Arslan, and M. Uysal, "Statistical modeling of propagation channels for terahertz band," in *Proc. 2017 IEEE Conference on Standards for Communications and Networking (CSCN)*, Helsinki, Finland, Sep. 2017, pp. 275–280.

[19] S. Kim and A. Zajic, "Statistical Modeling and Simulation of Short-Range Device-to-Device Communication Channels at Sub-THz Frequencies," *IEEE Trans. Wireless Commun.*, vol. WC-15, no. 9, pp. 6423–6433, Sep. 2016.